Sampling in x-ray ptychography

T. B. Edo,[1] D. J. Batey,[1] A. M. Maiden,[1] C. Rau,[2] U. Wagner,[2] Z. D. Pešić,[2] T. A. Waigh,[3] and J. M. Rodenburg[1,4]

[1]*Department of Electronic and Electrical Engineering, University of Sheffield, S1 3JD, United Kingdom*

[2]*Diamond Light Source Ltd., Harwell Science and Innovation Campus, Didcot, Oxfordshire OX 11 0DE, United Kingdom*

[3]*Photon Science Institute, University of Manchester, Oxford Road, Manchester, M13 9PL, United Kingdom*

[4]*Research Complex at Harwell, Harwell Oxford, OX11 0FA, United Kingdom*

(Received 28 March 2013; published 30 May 2013)

Coherent diffractive imaging (CDI) is a means of overcoming the resolution and image contrast limitations of electron and x-ray lenses. The central tenet of the method is that the intensity of the diffraction pattern must be measured on a sufficiently fine pixel pitch, which is inversely related to the size of the illuminated region of the object. We show here that ptychography—a form of CDI that uses many diffraction patterns—is not subject to this constraint. Using a variant of the ePIE inversion algorithm, we demonstrate experimentally that the sampling requirement in ptychography is independent of illumination size.

DOI: 10.1103/PhysRevA.87.053850 PACS number(s): 42.30.Kq, 42.30.Va, 42.30.Rx

I. INTRODUCTION

Since the first demonstration of x-ray diffractive imaging in 1999 using an iterative phase-retrieval algorithm [1], various implementations of the approach (see, for example, [2–6]) have attracted wide interest and extensive research. The principal advantage of the method is that it disposes of the need for refractive or diffractive lens optics: This is particularly advantageous for microscopic imaging using atomic-scale wavelengths (x-rays and electrons) where it is only possible to manufacture lenses of very small usable numerical aperture (of the order of 0.05).

In contrast to having lenses, which are rather poor, the experimental apparatus for diffractive imaging is extraordinarily simple. A specimen or object is illuminated by radiation and the intensity of the scattered waves is recorded on a two-dimensional detector. An algorithm of some type is then used to reconstruct an image of the object by solving for the phase of the diffraction pattern (given certain *a priori* knowledge about the object or the way that it was illuminated), thus creating a synthetic lens of high-numerical aperture (equivalent to the angle subtended by the detector at the object plane). Diffractive imaging therefore promises unsurpassed atomic-scale resolution, which is a key requirement in the understanding of many inorganic and biological structures.

Since its inception, an absolutely central tenet of diffractive imaging has been that the intensity of the diffraction pattern must be sampled at least at its Nyquist frequency. Since the diffraction pattern lies in reciprocal space, this sampling physically relates to the angular size of a detector pixel subtended at the object plane. Note that some authors have referred to this criterion as "oversampling" or "double sampling" because the Nyquist sampling of the intensity of the diffraction pattern is twice the requisite sampling of the underlying complex-valued wave function. Roughly speaking, this means that for a given detector in the Fraunhofer regime, the object or illumination incident upon the object must be smaller than a lateral size given by $D = \lambda L/2W$, where λ is the wavelength, L is the distance from the specimen to the detector plane, and W is the physical detector pixel pitch. This condition can be thought of as the minimum change in scattering angle necessary for the path length of waves emanating from opposite edges of the object (or illumination) to be $\lambda/2$.

We show here that for ptychography—a widely adopted form of diffractive imaging in which many diffraction patterns are collected from the specimen as it is moved to a number of positions relative to the illumination—this conventional wisdom relating to the sampling condition in reciprocal space does not apply. We demonstrate experimentally using visible light and x-rays that ptychographical diffraction patterns can be grossly undersampled, yet still give rise to satisfactory reconstructions. In fact, it would seem that the diffraction space sampling in ptychography is entirely independent of the illumination size: an astonishing result given the very extensive literature on diffractive imaging.

II. THE NYQUIST PTYCHOGRAPHIC SAMPLING CONDITION

Ptychography requires the recording of a number of diffraction patterns, each of which is collected from an area of the object delineated by a localized illumination function (often called a probe function). These areas are required to overlap with one another, thus furnishing the recorded dataset with a degree of redundancy. The object structure at any one point is expressed in two or more diffraction patterns, depending on how much the illuminated regions overlap with another. Clearly, as this overlap increases so does the redundancy in the recorded data. It is well established that this extra information can be used to good effect: to solve for the illumination function as well as the object function [7,8]; to solve for super-resolution diffraction data lying outside the detector area [9,10]; to recover experimental uncertainties such as errors in the position of probe [11–14]; and to reconstruct three-dimensional objects without rotating the specimen [15]. By simple number counting arguments [10], there is no mystery why it is possible to solve for so much more than the two-dimensional object function. The question of whether the diffraction pattern itself can be undersampled (and then retrieved), or what the fundamental ptychographic sampling actually is, is explored in the present work.

We write the complex wave field underlying the ptychographic dataset as the Fourier transform of the product of the

two-dimensional object function and an illumination function:

$$M(\boldsymbol{u},\boldsymbol{R}) = \int q(\boldsymbol{r})a(\boldsymbol{r}-\boldsymbol{R})\exp[2\pi\,\boldsymbol{u}\cdot\boldsymbol{r}]d\boldsymbol{r}, \qquad (1)$$

where $\boldsymbol{u}$ is a two-dimensional coordinate in reciprocal space (the Fraunhofer diffraction plane), $\boldsymbol{R}$ is a real-space two-dimensional vector coordinate (usually referred to as the probe position coordinate in the object plane), $q(\boldsymbol{r})$ is the specimen function, $a(\boldsymbol{r})$ is the illumination function, and $\boldsymbol{r}$ is a dummy real-space variable [16]. We now sample this physical function with a four-dimensional Dirac comb function: $\Delta_{U,R}(\boldsymbol{u},\boldsymbol{R}) \triangleq \delta(\boldsymbol{u}-\boldsymbol{u}_s,\boldsymbol{R}-\boldsymbol{R}_s)$, where the discrete coordinates $\boldsymbol{u}_s$ and $\boldsymbol{R}_s$ comprise integer multiples of the real- and reciprocal-space sampling periods U and R, respectively, i.e., $\boldsymbol{u}_s = (m\hat{\boldsymbol{u}}_x + n\hat{\boldsymbol{u}}_y)U$ and $\boldsymbol{R}_s = (p\hat{\boldsymbol{r}}_x + q\hat{\boldsymbol{r}}_y)R$; here m,n,p,q are integers, whereas $\hat{\boldsymbol{u}}_{x,y}$, $\hat{\boldsymbol{r}}_{x,y}$ represent unit vectors in the detector and specimen planes, respectively. The resulting sampled wave field is

$$M[\boldsymbol{u}_s,\boldsymbol{R}_s] = \int M(\boldsymbol{u},\boldsymbol{R})\Delta_{U,R}(\boldsymbol{u},\boldsymbol{R})d\boldsymbol{u}\,d\boldsymbol{R}. \qquad (2)$$

Although ptychography is all about solving the phase problem, it is informative to start by considering sampling in the case of the underlying complex wave impinging on the detector. We assume that the complex value of $M[\boldsymbol{u}_s,R_s]$ can be measured directly, which can then be referred to real space (the object plane) by taking its Fourier transform with respect to $\boldsymbol{u}_s$. Let us segment the specimen plane into a set of nonoverlapping square tiles of side R, and perform a ptychographic experiment in which a square illumination (probe) of side D is moved in steps of size R. Now when $D = R$, the entire specimen is spanned but there is no overlap and each square tile represents an independent experiment, with the sampling of its discrete Fourier transforms having the usual reciprocal relationship $U = 1/D$, which by definition is the exact Nyquist sampling. Clearly, the requisite Nyquist comb function for the entire dataset is therefore $\Delta_{1/R,R}(\boldsymbol{u},\boldsymbol{R})$, where

$$U = \frac{1}{R}. \qquad (3)$$

We investigate undersampling in the detector plane by increasing the physical probe size, while keeping the sampling function at the same intervals as defined in Eq. (3). With reference to Fig. 1, consider a square tile of the object of side R (the fixed probe movement sampling in real space): This is shown in red in both one dimension and two dimensions. If $D > R$, the detector pixel pitch U is now larger than the reciprocal of the probe size $(1/D)$. We can no longer obtain a true representation of the object function within any one tile by simply back Fourier transforming its phased diffraction pattern. Undersampling in the Fraunhofer diffraction plane means that areas of the object outside the tile wrap around and add to the opposite side of the tile. Areas of gray in Fig. 1(b) illustrate the parts of the object (within any given single tile) that have been corrupted by aliasing. Let us introduce a function $\alpha_U(\boldsymbol{r})$ that measures the nonuniqueness of the object estimate (due to aliasing) within a tile. Since the aliased object function is made up of the sum of n cyclic views, we can define the ambiguity at coordinate $\boldsymbol{r}$ as $\alpha_U(\boldsymbol{r}) = 1/n$, where n is the (integer) number of times the object estimate has been superimposed upon itself at the position $\boldsymbol{r}$. In Figs. 1(b) and 1(c), the probe is delineated by the outer rectangle (solid green box of size D). The light shaded areas show where $\alpha_U(\boldsymbol{r}) = 1/2$, and the darker regions are where $\alpha_U(\boldsymbol{r}) = 1/4$. We can define another function, $\pi_R(\boldsymbol{r})$, which enumerates the number of diffraction patterns to which a particular element of the object positioned at $\boldsymbol{r}$ contributes [see Fig. 1(c)]. By using these functions, $\alpha_U(\boldsymbol{r})$ and $\pi_R(\boldsymbol{r})$, we can identify the Nyquist sampling limit in the overlapping configuration of the simplified square geometry using the condition $\alpha_U(\boldsymbol{r})\pi_R(\boldsymbol{r}) = 1$. In other words, at least in terms of information content, the effect of the ambiguity introduced by undersampling the diffraction pattern is exactly compensated by the additional redundancy due to the overlap of the illumination positions. This argument is also valid for other geometries where the probe has an arbitrary shape, as long as the probe fills the primary real-space window defined by R.

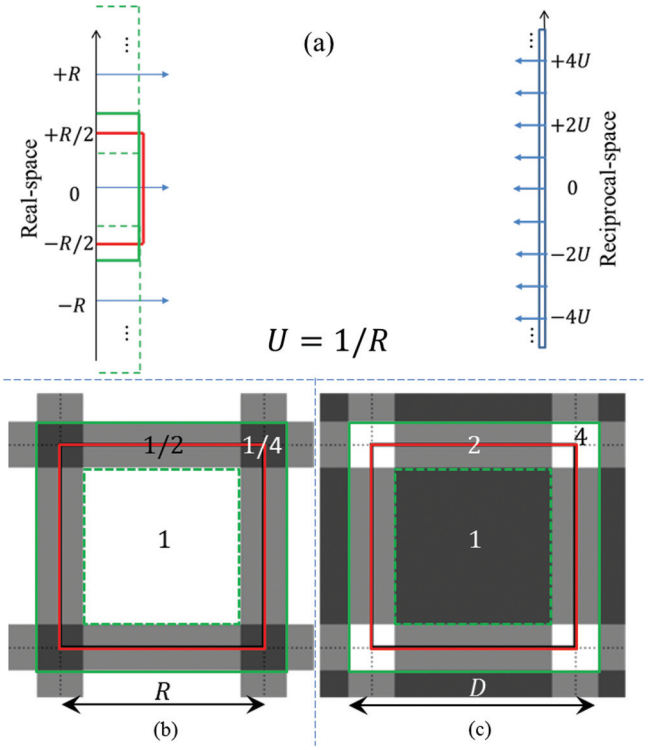

FIG. 1. (Color online) Illustration of the conservation of information density in the specimen plane in ptychography. (a) shows the Nyquist sampling limit in a one-dimensional case, where the sampling points in both real and reciprocal space are specified by the four-dimensional Dirac comb function $\Delta_{U,R}(\boldsymbol{u},\boldsymbol{R})$. As the illumination size is increased from $D = R$ in the nonoverlapping configuration (red rectangle) to $D > R$ in the overlapping configuration (solid green rectangle), aliasing due to undersampling creates cyclically overlapping regions where the solution is ambiguous. These regions are illustrated in (b) by $\alpha_U(\boldsymbol{r}) = 1/2$ in the case involving two cyclically overlapping areas and by $\alpha_U(\boldsymbol{r}) = 1/4$ at the edge where the solution comprises the sum of four cyclically overlapping areas of the specimen. At the same time, the linear overlapping regions from adjacent illumination positions in ptychography [see (c)] provide additional constraints for the solution in the aliased region via $\pi_R(\boldsymbol{r})$. Consequently, the Nyquist limit may also be expressed by the equation $\alpha_U(\boldsymbol{r})\pi_R(\boldsymbol{r}) = 1$.

In the real experiment we undertake in Sec. IV, the probe positions are offset by a random amount, as is usual practice, to help reduce the emergence of periodic artifacts in the recovered object and probe functions [17]. This random offset in probe positions is detrimental at the Nyquist sampling limit because any departure of the sampling function from $\Delta_{U,R}(\boldsymbol{u},\boldsymbol{R})$ results in a situation where $\alpha_U(\boldsymbol{r})\pi_R(\boldsymbol{r}) < 1$ and as a result the corresponding ptychographic dataset cannot exactly compensate for aliasing—we note, however, that this situation can be remedied by decreasing the average step size $\overline{R}$ until the condition $\alpha_U(\boldsymbol{r})\pi_{\overline{R}}(\boldsymbol{r}) \geqslant 1$ is again satisfied for all real-space points.

However, even bearing in mind that we are assuming the diffraction pattern can be measured in modulus and phase, there is no guarantee that a unique solution can be found for the object function, since having exactly the same number of equations as unknowns is not the same as proving that a solution exists. We find that when an unmodified inversion algorithm such as ePIE [8] is run on data that fulfills Eq. (3), but does not satisfy the sampling condition in the detector plane (i.e., when $D > R$, so that $U > 1/D$), then there is no convergence to the correct solution. At points in the regions of overlap, the calculated exit wave at each iteration is the product of a wrapped-around probe function (due to periodic continuation) and a wrapped-around object tile. The update function does not separate these mixed up components, so this particular solution method fails.

Nevertheless, we conjecture that the relationship expressed in Eq. (3) together with the simple connection between aliasing the ptychography illustrated in Fig. 1 are sufficient to ensure that a unique solution is found at the Nyquist limit (in the case of complex measurements), because the configuration of diffractive imaging systems guarantees that no two measurements corresponding to different values of $\boldsymbol{u}_s$ and $\boldsymbol{R}_s$ encode the same information about the specimen. That is to say, their underlying measurement basis (complex exponential modified by the form of the shifted illumination) never points in exactly the same Hilbert-space direction so that their collection spans the space. Below we introduce a modified version of ePIE that can indeed cope with gross undersampling in the diffraction plane. We will show that the probe overlap redundancy can in practice be used to compensate fully for diffraction pattern undersampling.

Before we proceed, it is useful to introduce some dimensionless variables that characterize how much a given ptychography experiment has been over- or undersampled. Remember that this must take into account both the sampling in the detector plane (U) and the sampling in real space (the probe movement distance, R). We will call the condition in Eq. (3) the "fundamental ptychographic sampling"—or FPS: We emphasize that this has been derived assuming the diffraction patterns are measured in modulus and phase and where the field of view is of infinite extent.

The FPS intervals in reciprocal and real space are equal to the reciprocal of one another; hence $UR = 1$. Since in a real experiment, the values of U and R can be changed independently, the value of their product differs from unity when the dataset is either oversampled or undersampled relative to the FPS. To oversample the dataset, we decrease the value of R while keeping U fixed or decrease the value of U while keeping R fixed (or both). Thus the amount of oversampling along either the x or y direction is inversely proportional to the product of these sampling intervals and is quantified by the one-dimensional sampling ratio

$$S_{x,y} = \frac{1}{UR}. \tag{4}$$

The amount of oversampling or undersampling for the entire ptychographic dataset is given by the sampling ratio S_Π, which is the product of the one-dimensional sampling ratios along the x and y directions, i.e., $S_\Pi = S_{x,y}^2$, so that

$$S_\Pi = \left(\frac{1}{UR}\right)^2. \tag{5}$$

The FPS requirement for the wave field in Eq. (2) occurs when $S_\Pi = 1$, with $S_\Pi > 1$ and $S_\Pi < 1$ corresponding to over- and undersampling, respectively. In a real experiment, the reciprocal-space sampling interval is determined by the detector sampling pitch W, the wavelength of the radiation λ, and the distance from the specimen plane to the detector plane, L, via the relationship $U = W/\lambda L$ for the Fraunhofer regime, giving

$$S_\Pi = \left(\frac{\lambda L}{WR}\right)^2. \tag{6}$$

The main benefit of Eq. (6) is that it can be used to compute the sampling ratio from parameters that are readily accessible from experiments without the need to estimate the size of the illumination, which is particularly difficult for a soft edge illumination function, of the type that is employed in the experimental section of this paper. However, the expression in Eq. (6) does not immediately highlight the means via which real-space oversampling relaxes the reciprocal-space sampling requirement. For this, the sampling ratio needs to be expressed using dimensionless illumination-dependent parameters, such as the coherent diffractive imaging (CDI) oversampling ratio $\sigma_{x,y}$—given by $(UD)^{-1}$, a similar expression to Eq. (4)—and the overlap parameter of ptychography, $\varpi_{x,y}$—given by $(1 - R/D)$. Consequently, the real- and reciprocal-space sampling intervals can be written as $R = D(1 - \varpi_{x,y})$ and $U = (D\sigma_{x,y})^{-1}$, respectively, where the size of the illumination now serves as the basic unit of measurement. In this nomenclature, the sampling ratio is

$$S_\Pi = \left(\frac{\sigma_{x,y}}{1 - \varpi_{x,y}}\right)^2, \tag{7}$$

where the range of the CDI oversampling ratio is $0 < \sigma_{x,y} < 2$ and the range of the overlap parameter of ptychography is $0 < \varpi_{x,y} < 1$.

The fact that we have a phase problem suggests that we need at least two times as many measurements to obtain a reconstruction ($S_\Pi > 2$). In fact, we find below that in favorable circumstances (cases where the probe is highly structured) we can experimentally reconstruct an object when $S_\Pi < 1$; a very surprising result. This suggests that the sampling requirement (and thus oversampling) is one facet of the phase problem that should be decoupled from the contributions due to probe structure, since the form of the probe (which is clearly independent of the sampling condition)

impacts on the quality of the reconstruction. Furthermore, the quality of the reconstruction is also dependent on the field of view, since perimeter areas in a finite field of view have reduced redundancy. In light of these complications, the FPS is useful because it provides the means to decouple the effect of sampling from other aspects of the phase problem that impact on the quality of the reconstruction, so that they can be further investigated in isolation. Its precise definition means it can be used to compare quantitatively the ptychographic sampling in different experimental configurations.

III. A RECONSTRUCTION ALGORITHM FOR SPARSE DIFFRACTION PATTERNS

We examine in this paper the case of recovering ptychographic reconstructions from "sparse" diffraction patterns. In a physical experiment, it will normally be the case that the detector pixels are closely packed, so that if the diffraction pattern is undersampled, a significant region of intensity structure in the diffraction pattern will contribute to a given single measured data value. Here we confine ourselves to the situation where the detector pixels are small, but separated by large gaps. In this way, we examine the issue of sampling and information content *per se*, and thus demonstrate that the FPS periodicity in real and reciprocal space does indeed apply and that the degree of probe overlap balances the ambiguities introduced by undersampling in the detector plane. With reference to Fig. 2, the square grid represents the pixels at the detector plane of a ptychographic experiment. The grid itself satisfies the sampling criterion ($U \approx 1/2D$—the factor of $1/2$ allows the algorithm to cope with soft edged illumination, because a larger real-space window minimizes the effect of aliasing during iterative calculations). In the calculations and experiments that follow, we discard the black pixels, leaving a sparsely and undersampled diffraction pattern, with measurements only made at the white pixels. Since U and R can be traded for one another without loss of information at the FPS limit, this means that as long as $S_\Pi > 2$ for intensity measurements, the value of the wave field in the black pixel region should be dependent on the measured data across the entire dataset and can thus be recovered.

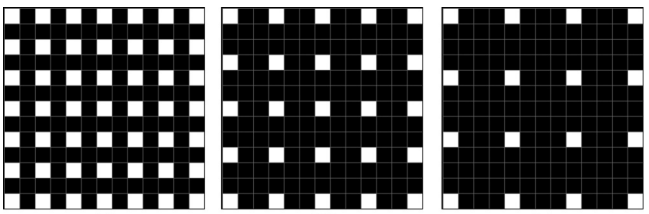

FIG. 2. Illustration of detector plane undersampling. The white boxes represent pixels with measured intensities and black boxes represent pixels with no information. The algorithm recovers phase of the wave field in regions represented by the white boxes and also solves for the complex-valued wave field in the regions represented by black boxes. (a) represents the case where the diffraction pattern is undersampled over the two dimensions by a factor of 4, whereas (b) and (c) represent the cases for undersampling factors of 9 and 16, respectively.

To achieve the requisite "up-sampling" process, we use a modified version of the ePIE algorithm. It has been shown elsewhere [9,10] that super-resolution data residing outside the detector can be recovered by allowing unmeasured regions to "float". That is to say, the Fourier modulus constraint is only applied to the pixels that have been measured. Whatever modulus (and phase) that is derived from the forward propagation calculation at unmeasured pixels remains untouched. As long as the experiment is sufficiently overconstrained, the unmeasured pixels should converge to their correct value. In the present context, the value of the wave field in the black pixel regions of Fig. 2 is allowed to float: Its running estimate is retained in phase and modulus. We have shown that information content lost by under-sampling in the diffraction plane is balanced by redundancy in the probe area overlap. This strategy is therefore a way of allowing that redundancy to reduce the necessary sampling in the detector plane. We will call this algorithm floating-PIE (or f-PIE).

IV. EXPERIMENTAL TESTS

We test the limits of ptychographic sampling using both hard x rays and visible light. X-ray experiments were performed at the Diamond Light Source on the I13 beamline [18], which is unusually long (250 m) so as to provide for very large transverse coherence lengths (about 100×800 μm). The monochromated x-ray energy E was 8.7 keV, with $\Delta E/E = 10^{-4}$. Since the largest path length difference in the experimental set-up described below is about 150λ, we can therefore assume the coherence width is sufficiently large to guarantee that the diffraction data is fully coherent. The beam illuminated a test object consisting of 28-μm-diameter M-270 amine superparamagnetic dynabeads mounted on a transmission electron microscopy grid with a thin amorphous carbon support film. The illumination size at the object plane was first checked by direct observation using a phosphor screen, and then reconstructed using the f-PIE algorithm. The detector, a MaxiPix TAA22PC with a pixel pitch of 55 μm, was mounted 14.62 m downstream from the sample. The dataset comprises 1024 diffraction patterns generated using a 32×32 raster scan of the specimen with an average step size (real-space sampling) of 5.8 μm (with small known random offsets of up to ± 0.3 μm to avoid the raster pathology) and a reciprocal-space sampling pitch of 26.9 mm^{-1} ($U = W/\lambda L$). The setup for the x-ray experiment is shown in Fig. 3.

The f-PIE algorithm was used to process four datasets, each with different sampling ratios, derived from the measured diffraction patterns. These four datasets contain diffraction patterns that were undersampled by factors of 1, 4, 9, and 16, respectively, giving sampling-ratio parameters for the dataset shown in Table I. The first column of Table I shows the amount of diffraction pattern oversampling, which is governed by the reciprocal-space sampling-ratio (or CDI sampling-ratio) parameter. The second column shows the real-space sampling ratios, which govern the amount of real-space oversampling due to the ptychographic overlap; this value is a constant in all of these experiments because we only undersample the dataset in reciprocal space. The final column shows the amount of oversampling for the entire ptychographic dataset.

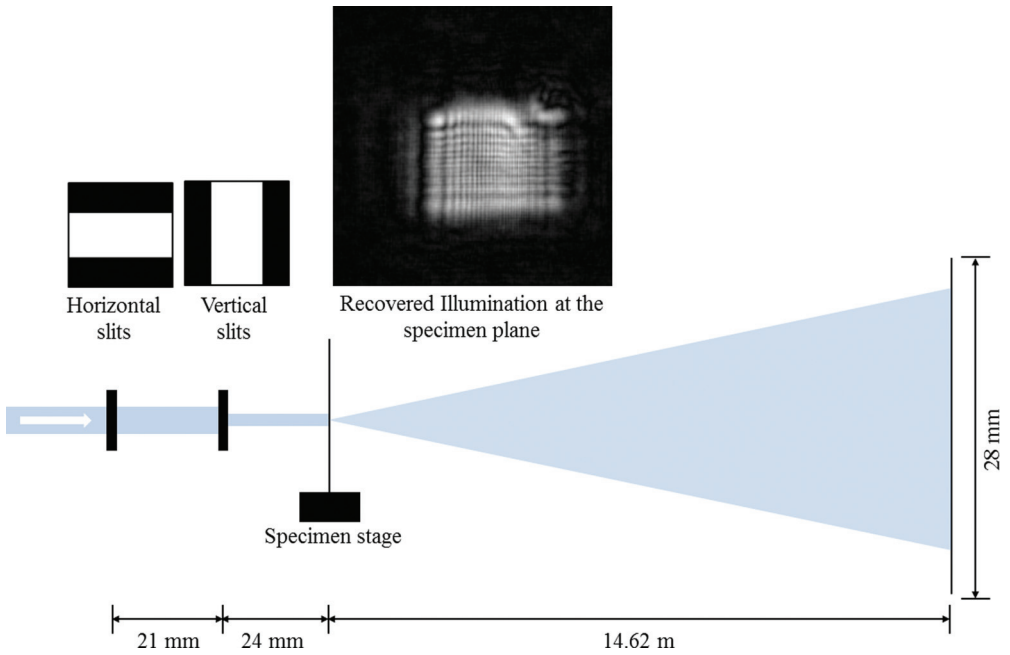

FIG. 3. (Color online) Experimental setup for x-ray ptychography. The specimen was illuminated by an x-ray beam that was formed with the two sets of horizontal and vertical slits shown in the figure.

The diffraction patterns were inputted to the f-PIE algorithm using the up-sampling scheme in Fig. 2. The outputs of the f-PIE algorithm calculations after 200 iterations are shown in Fig. 4. These results demonstrate that it is possible to obtain a reasonable x-ray ptychographic reconstruction from diffraction data which has been undersampled—in terms of lost two-dimensional data—by a factor of 9 relative to conventional single shot CDI.

However, in this first experiment we have used a very simple illumination function. It is well known that when the illumination has a complicated form, the ptychographic inversion is more constrained. To demonstrate much more radical undersampling in the diffraction data, we perform a second experiment using visible light in the so-called super-resolution geometry [10], employing a strong spatial diffuser to add random diversity into the illumination.

With reference to Fig. 5, the illumination is formed by propagating the image of a 100-μm pinhole—which is covered with a diffuse plastic film—3.17 mm to the specimen plane.

TABLE I. Illustration of the distribution of the amount of sampling between real and reciprocal space in the x-ray experiment. S_Π was calculated using Eq. (6). Furthermore, we assume that $\sigma_{x,y} = 1$ when the diffraction data was just sufficiently sampled according to the CDI criterion.

$\sigma^2_{x,y}$ [a]	$(1 - \varpi_{x,y})^{-2}$ [b]	S_Π [c]
1	41	41
1/4	41	10
1/9	41	4.6
1/16	41	2.6

[a]Reciprocal-space sampling ratio.
[b]Real-space sampling ratio.
[c]Ptychography sampling ratio.

The specimen (a resolution test target) was mounted on a computer-controlled motorized x/y stage, which translated the specimen laterally by a step size of $\sim$50 μm to a grid of 20×20 positions, wherefrom 400 diffraction patterns were recorded. The data were recorded with a 16-bit AVT Pike

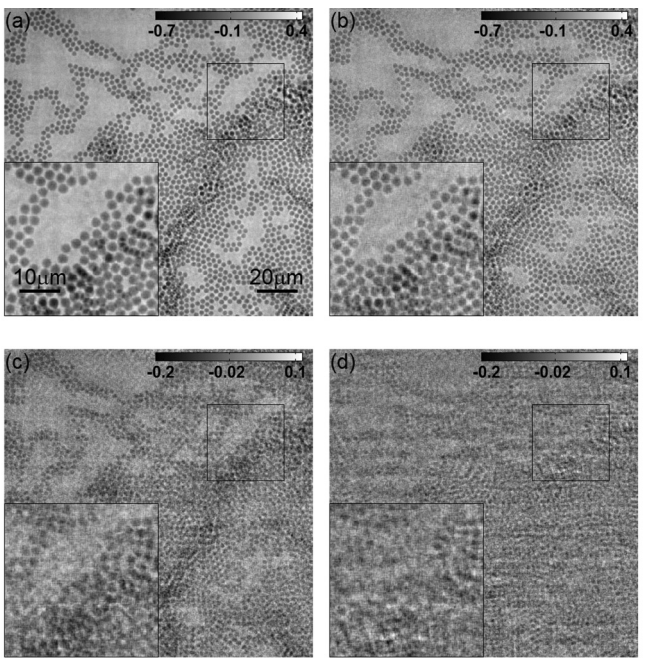

FIG. 4. X-ray ptychographic reconstructions using a set of undersampled diffraction patterns. The images in (a)–(d) represent the output of the algorithm for datasets with a two-dimensional diffraction pattern undersampling of 1, 1/4, 1/9, and 1/16, respectively, corresponding to ptychographic sampling ratios of $S_\Pi = 41$, $S_\Pi = 10$, $S_\Pi = 4.6$, and $S_\Pi = 2.6$.

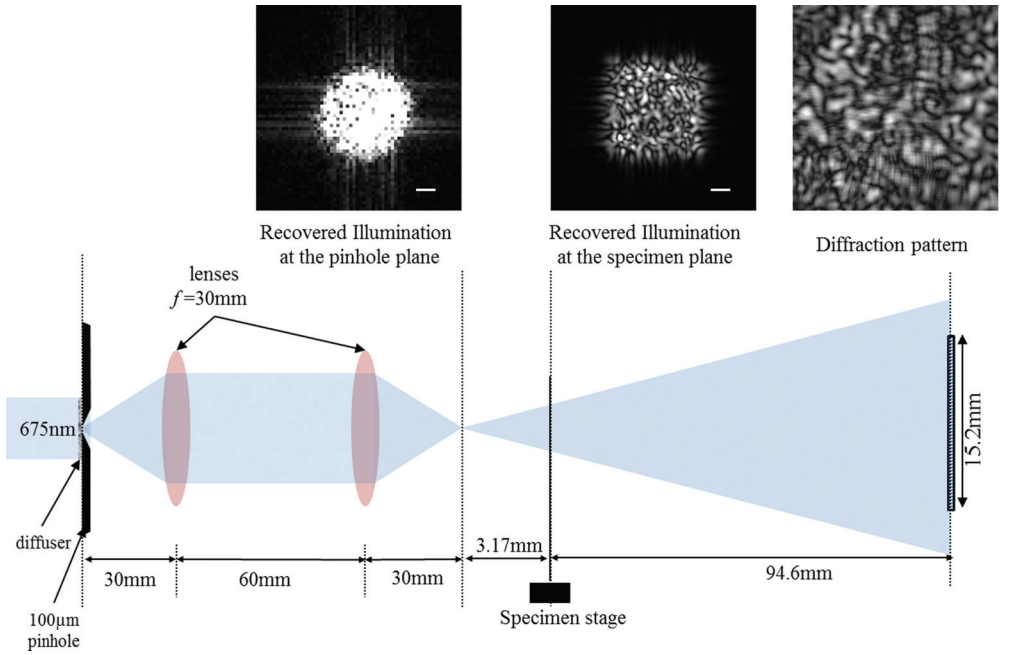

FIG. 5. (Color online) Experimental setup used to demonstrate the gross reciprocal-space undersampling that can be tolerated in ptychography when there is a large amount of illumination area overlap and high illumination diversity. The size of the scale bars at the pinhole and specimen planes are 25 and 100 μm, respectively. See text for further details.

F421F detector (comprising 2048 × 2048 pixels of 7.4 μm pixel pitch) placed 94.6 mm downstream from the specimen plane. The maximum sampling pitch above which a significant amount of aliasing crops into the real-space representation of the illumination was eight times this detector pixel pitch. All the diffraction patterns were therefore first undersampled by a factor of 8 to 256 × 256 pixels to serve as the reference dataset.

The reference diffraction patterns (256 × 256 pixels) from the visible light setup of Fig. 5 were then undersampled by factors of 1, 4, 16, 64, 256, and 1024 to generate datasets with sampling parameters shown in Table II. Comparing the sampling ratios for the reference datasets of both experiments ($S_\Pi = 41$ for x-ray and $S_\Pi = 465$ for visible light) shows that the visible light setup has a much higher sampling ratio and is thus expected to produce higher quality reconstructions for calculations that process diffraction patterns with the same amount of reciprocal-space undersampling. Figure 6 shows the

TABLE II. Illustration of the distribution of the amount of sampling between real and reciprocal space in the visible light experiment. S_Π was calculated using Eq. (6) and we again make the assumption that $\sigma_{x,y} = 1$ for the reference dataset where the reciprocal-space sampling is only just fulfilled.

$\sigma^2_{x,y}$	$(1 - \varpi_{x,y})^{-2}$	S_Π
1	465	465
1/4	465	116
1/9	465	29
1/16	465	7.3
1/256	465	1.8
1/1024	465	0.5

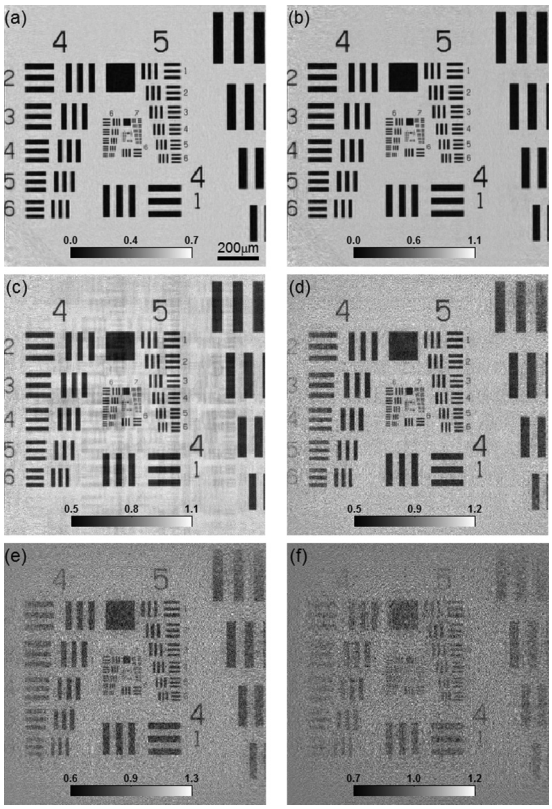

FIG. 6. Results from the f-PIE algorithm after 100 iterations. The images in (a)–(f) represent the output of the algorithm for datasets with two-dimensional diffraction plane undersampling ratios of 1, 1/4, 1/16, 1/64, 1/256, and 1/1024, respectively; corresponding to $S_\Pi = 465$, $S_\Pi = 116$, $S_\Pi = 29$, $S_\Pi = 7.3$, $S_\Pi = 1.8$, and $S_\Pi = 0.5$.

output images from the f-PIE algorithm after 100 iterations of processing these different datasets. Diffraction patterns undersampled by a factor of 4 and greater still give a good quality reconstruction, as expected given the high sampling ratios.

Surprisingly, the results also show that the reconstruction does not completely break down as the sampling ratio decreases below 2, and still gives a recognizable image at a sampling ratio of 0.5. We should recall that a sampling ratio of 1 in theory applies only when diffraction patterns are complex variables—half the sampling expected when we measure intensity. In other words, a sampling ratio of 0.5 has undersampled the recorded intensity by a factor of 4. Clearly, the information content of these images is less straightforward than simply the number of pixels they contain. We might suppose that the test object has favorably low information content and that the diversity in the illumination interacts with the sparse sampling in a way that leads to a form of compressive sensing [19]. These issues clearly require further work.

V. DISCUSSIONS AND CONCLUSION

We have demonstrated experimentally that the sampling requirement in the detector plane of an x-ray ptychographic diffractive imaging experiment bears no relationship to the usual oversampling condition in a conventional CDI experiment (where only one diffraction pattern is processed). A simple geometric construction with a square probe was first used to show that in the absence of the phase problem, information content in ptychography is wholly independent of the probe size (illumination area). Reducing the probe movement step size R—thus increasing the sampling periodicity in real space (sometimes expressed as the degree of overlap)—relaxes the sampling periodicity in the diffraction plane U. As long as the simple reciprocal relationship $R = 1/U$ is satisfied, then the probe can be of any size greater than or equal to R. We call this condition the FPS. We would expect that in an actual experiment the minimum sampling should need to be substantially increased beyond the FPS to obtain a meaningful image, if nothing else because measuring only intensity will introduce at least a further factor of 2 in the number of diffraction pixels or probe positions required. In fact we have shown here experimentally (using visible-light optics) that in favorable circumstances we can obtain recognizable reconstructions of the object with a sampling of half that of the FPS.

These demonstrations have been undertaken using a variant of the ePIE algorithm wherein sparsely sampled ptychographic diffraction patterns can be up sampled in order to access the probe-position redundancy data in the object plane. We used this successfully with experimental hard x-ray and visible-light data to up sample diffraction patterns in any one linear direction by a factor of 4 for x rays and 32 in the case of light; corresponding to retrieving a factor of 16 and 1024 times as much data over that selected from the two-dimensional detector.

These results raise many new interesting questions. How can we solve a phase problem when we have fewer measurements than unknown variables? In the case we demonstrate here, this is almost certainly due to the simple and sharp structure of the object we are using in the optical experiments and the very high diversity in the structure of the illumination. We conjecture that the combination of the experimental setup and the processing scheme has fortuitously led to a form of compressive sensing, at least in the case of the extreme undersampling of the visible-light data. Understanding the exact interplay of the probe shape, object structure, and requisite sampling is a complex problem. However, the key conclusion of this work is that when we think of sampling in diffractive imaging, the central tenet of conventional CDI—the principle of oversampling which has dominated the whole rationale of the subject since its inception 14 years ago—simply does not apply to ptychography. In ptychography, the illumination size does not matter.

ACKNOWLEDGMENTS

This work was funded by the EPSRC Doctoral Prize Fellowship and the EPSRC Basic Technology Grant No. EP/E034055. The authors thank Phase Focus Ltd. for access to a Phase Focus optical ptychographical microscope.

[1] J. Miao, P. Charalambous, J. Kirz, and D. Sayre, Nature (London) **400**, 342 (1999).
[2] V. Elser, J. Opt. Soc. Am. A **20**, 40 (2003).
[3] H. H. Bauschke, P. L. Combettes, and D. R. Luke, J. Opt. Soc. Am. A **20**, 1025 (2003).
[4] G. Oszlanyi and A. Suto, Acta Crystallogr., Sect. A: Found. Crystallogr. **60**, 134 (2004).
[5] D. R. Luke, Inverse Probl. **21**, 37 (2005).
[6] Marchesini, Rev. Sci. Instrum. **78**, 011301 (2007).
[7] P. Thibault, M. Dierolf, A. Menzel, O. Bunk, C. David, and F. Pfeiffer, Science **321**, 379 (2008).
[8] A. M. Maiden and J. M. Rodenburg, Ultramicroscopy **109**, 1256 (2009).
[9] T. B. Edo, F. Zhang, and J. M. Rodenburg, Proc. SPIE Scanning Microsc. **7729**, 77291H (2010).
[10] A. M. Maiden, M. J. Humphry, F. Zhang, and J. M. Rodenburg, J. Opt. Soc. Am. A **28**, 604 (2011).
[11] A. C. Hurst, T. B. Edo, T. Walther, F. Sweeney, and J. M. Rodenburg, J. Phys.: Conf. Ser. **241**, 012004 (2010).
[12] M. Guizar-Sicairos and J. R. Fienup, Opt. Express **17**, 2670 (2009).
[13] A. Shenfield and J. M. Rodenburg, J. Appl. Phys. **190**, 124510 (2011).
[14] A. M. Maiden, M. J. Humphry, M. C. Sarahan, B. Kraus, and J. M. Rodenburg, Ultramicroscopy **20**, 64 (2012).

[15] A. M. Maiden, M. J. Humphry, and J. M. Rodenburg, J. Opt. Soc. Am. A **29**, 1606 (2012).
[16] J. M. Rodenburg, Adv. Imaging Electron Phys. **150**, 87 (2008).
[17] P. Thibault, M. Dierolf, O. Bunk, A. Menzel, and F. Pfeiffer, Ultramicroscopy **190**, 338 (2009).
[18] C. Rau, U. Wagner, Z. Pesic, and A. De Fanis, Phys. Status Solidi A **208**, 2522 (2011).
[19] E. J. Candes, M. B. Wakin, IEEE Signal Process. Mag. **25**, 21 (2008).